Biogeosciences Discuss., 8, 4239–4280, 2011
www.biogeosciences-discuss.net/8/4239/2011/
doi:10.5194/bgd-8-4239-2011

Biogeosciences Discussions

Climate impacts on the structures of the North Pacific air-sea CO_2 flux variability

V. Valsala[1], S. Maksyutov[1], M. Telszewski[1], S.-I. Nakaoka[1], Y. Nojiri[1], M. Ikeda[2], and R. Murtugudde[3]

[1]CGER, National Institute for Environmental Studies (NIES), Tsukuba, Japan
[2]Retired from EES, Hokkaido University, Japan
[3]ESSIC, University of Maryland, College Park, MD, USA

Received: 5 April 2011 – Accepted: 20 April 2011 – Published: 2 May 2011

Correspondence to: V. Valsala (vinu.valsala@nies.go.jp)

Published by Copernicus Publications on behalf of the European Geosciences Union.

Abstract

Some dominant spatial and temporal structures of the North Pacific air-sea CO_2 fluxes in response to the Pacific Decadal Oscillation (PDO) are identified in four data products from four independent sources: an assimilated CO_2 flux product, two forward model solutions, and a gridded pCO_2 dataset constructed with a neural network approach. The interannual variability of CO_2 flux is found to be an order of magnitude weaker compared to the seasonal cycle of CO_2 flux in the North Pacific. A statistical approach is employed to quantify the signal-to-noise ratio in the reconstructed dataset to delineate the representativity errors. The dominant variability with a signal-to-noise ratio above one is identified and its correlations with PDO are examined. A tentative four-box structure in the North Pacific air-sea CO_2 flux variability linked to PDO emerges in which two positively correlated boxes are oriented in the northwest and southeast directions and contrarily, the negatively correlated boxes are oriented in the northeast and southwest directions. This pattern is verified with the CO_2 and pCO_2 from four products and its relations to the interannual El Niño-Southern Oscillation (ENSO) and lower-frequency PDO are separately identified. A combined EOF analysis between air-sea CO_2 flux and key variables representing ocean-atmosphere interactions is carried out to elicit robust oscillations in the North Pacific CO_2 flux in response to the PDO. The proposed spatial and temporal structures of the North Pacific CO_2 fluxes are insightful since they separate the secular trends of the surface ocean carbon from the interannual variability. The regional characterization of the North Pacific in terms of PDO and CO_2 flux variability is also instructive for determining the homogeneous oceanic domains for the Regional Carbon Cycle and Assessment Processes (RECCAP).

1 Introduction

The ocean absorbs nearly one third of the anthropogenic CO_2 from the atmosphere via air-sea gas exchange (Gruber et al., 2009). The ocean's uptake of anthropogenic

BGD
8, 4239–4280, 2011

CO_2 has significantly contributed to the mitigation of the net growth of CO_2 in the atmosphere. The annual mean value of oceanic sink of CO_2 was nearly zero during the pre-industrial era (i.e., when the atmospheric CO_2 concentration was at 273 parts per million; ppm) and rose fairly rapidly beyond 1.5 petagram of carbon (Pg C; i.e., when the atmospheric CO_2 concentration rose to over 380 ppm and continues to rise). The contemporary CO_2 sink of the ocean, which includes both natural and anthropogenic fractions, is estimated to be between 1.5 and 2.2 Pg C (e.g., Takahashi et al., 2009; Gruber et al., 2009; Le Quéré et al., 2007).

The oceanic sinks of CO_2 respond to the climate anomalies. In addition to the climate induced variability, the secular trends in the sinks due to the accumulation of CO_2 in the atmosphere cause significant deviations in the annual mean value mentioned above. From the previous studies, it has been estimated that 70% of the interannual variability of contemporary air-sea CO_2 fluxes is driven by the cycles of El Niño-Southern Oscillation (ENSO) in the Pacific, namely a positive sink or an anomalous reduction in oceanic outgassing of ~ 0.5 Pg C during ENSO years (Valsala and Maksyutov, 2010; Gruber et al., 2009; McKinley et al., 2004; Obata and Kitamura, 2003; Le Quéré et al., 2000). It should be noted that ENSO has a global reach in terms of temperature and precipitation teleconnections and the phasing of marine vs. terrestrial sources/sinks have yet to be fully understood (Jones et al., 2001). The majority of the remaining variability in CO_2 sink is driven by the Southern Annular Mode (SAM; Le Quéré et al., 2007; Lovenduski et al., 2007). In addition to this interannual variability, the contemporary air-sea CO_2 fluxes also show interdecadal variability related to the Pacific Decadal Oscillations (PDO; see Mantua et al., 1997) and the North Atlantic Oscillations (NAO; see Hurrell, 1995 for NAO; impacts on oceanic carbon cycle are reported by several studies – Thomas et al., 2008; McKinley et al., 2006; Patra et al., 2005). Moreover, because of the accumulation of CO_2 in the atmosphere and subsequent changes in the dynamics of the atmosphere and the ocean, regional air-sea CO_2 fluxes also display clear trends (Le Quéré et al., 2007, 2009).

BGD
8, 4239–4280, 2011

The above conclusions on interannual variability of air-sea CO_2 fluxes are drawn mainly from simulations of simple-to-intermediate complexity, state-of-the-art, biogeochemical general circulation models (BGCMs). A few studies have validated these results with the data-model intercomparison based on available observations. For instance, the general conclusions on ENSO and air-sea CO_2 flux relations in the tropical Pacific were observationally verified by Feely et al. (2002; also see Christian et al., 2008). Similarly, the southern ocean trends of CO_2 emissions are also backed by observations in the work of Le Quéré et al. (2007) and Metzl et al. (2006). However, the limited number of observations in terms of spatial and temporal dimensions make it rather difficult to determine the robustness of these conclusions, especially when one wants to separate the effect of interannual to interdecadal variability from the secular trends or delineate the impacts of ocean dynamics (e.g., thermocline variability) and thermodynamics (mixed layer and sea surface temperature variability) on air-sea CO_2 and sea water partial pressure of CO_2 (pCO_2) variations.

The methods for estimation of air-sea CO_2 fluxes on global scale can be generally categorized as follows: (1) direct observations of global surface ocean pCO_2 are interpolated onto the global domain and the products typically include climatological maps of air-sea CO_2 fluxes, as in the database of Takahashi et al. (2009). Due to the limited number of observations of pCO_2 especially at interannual time scales, this method does not yield the vital information regarding the interannual to interdecadal variability of air-sea CO_2 fluxes. (2) State-of-the-art BGCMs incorporating ecosystem models of varying complexities are employed in order to simulate global ocean CO_2 fluxes on interannual to interdecadal time scales (Christian et al., 2008; McKinley et al., 2004; Obata and Kitamura, 2003, Le Quéré et al., 2000). (3) Inverse estimations are made from transports of atmospheric CO_2 concentrations and are utilized to generate global air-sea CO_2 fluxes on interannual time scales (Patra et al., 2005; Gurney et al., 2004; Rödenbeck et al., 2003). However the regional patterns of interannual variability are poorly resolved in these rather coarse resolution inversion systems (Gurney et al., 2004). (4) The BGCMs as well as atmospheric transport models are optimized

BGD
8, 4239–4280, 2011

with various sets of observations and a robust estimation of air-sea CO_2 fluxes are attempted (Valsala and Maksyutov, 2010; Tjiputra et al., 2007; Baker et al., 2006). (5) The empirical relations between certain surface ocean parameters and pCO_2 are exploited in order to infer the pCO_2 on interannual time scales (Telszewski et al., 2009, 2011; Park et al., 2010). In this study, we use air-sea CO_2 fluxes estimated with some of the methods discussed above and examine the patterns of interannual variability of North Pacific CO_2 fluxes and the possible climatic control from interannual (ENSO) to decadal (PDO) time-scales.

A most comprehensive and commendable study on the interannual variability of air-sea CO_2 fluxes in the North Pacific and its linkage to PDO was carried out by McKinley et al. (2006). In their study, they compared results from seven biogeochemical models, each of them with a varying complexity of ecosystem models, and examined the interannual variability of North Pacific air-sea CO_2 fluxes. A major conclusion of their study was that the magnitude of low-frequency air-sea CO_2 flux variability in the North Pacific is relatively small, with a maximum of amplitude of 0.025 Pg C yr^{-1} related to PDO. The reason for such a weak decadal variability is that the effect of decadal sea surface temperature (SST), dynamics of dissolved inorganic carbon (DIC) as well as alkalinity on pCO_2 are opposite in phase and similar in magnitude. Therefore, the net change in pCO_2 due to the sum of partial changes induced by above three factors nearly cancel each other leaving a relatively small net residual of interannual pCO_2 anomalies (and thereby a weak air-sea CO_2 flux interannual anomaly as well). Even though the net interannual variability naturally appears as a small residual of the above controlling factors, it is still worth considering because such anomalies should be separated first from the secular trends related to the natural modes of variability in order to assess the growth rate of CO_2 in the ocean due to anthropogenic forcing. This is also critical for understanding the response of this important region to continued anthropogenic forcing.

Although the study by McKinley et al. (2006) was quite comprehensive, in the sense that it assembled the results from seven biogeochemical models, the conclusions

BGD
8, 4239–4280, 2011

drawn thereby were fairly general. The study was based on a suite of forced ocean models with very little direct comparison with observations. Moreover, the study lacked the presentation of a close look into the spatio-temporalvariability of the North Pacific air-sea CO_2 fluxes with respect to PDO. This is important to investigate because the crucial information for identifying the secular trends of CO_2 in the ocean from the sparse observations is even more important in the context of global warming and its potential impacts on ocean's ability to take up CO_2. It is important to avoid confusing such trend analysis with the natural interannual and interdecadal variability of CO_2 fluxes. To identify the regional patterns of the North Pacific CO_2 fluxes in response to PDO is the major goal of our study. We also strive to quantify the dynamical and thermodynamical contributions to the net CO_2 variability. Much attention has been focused on the impact of PDO on ecosystem responses in terms of regime shifts (for ex., Chavez et al., 2002; Mantua et al., 1997) and the role of bottom-up (circulation changes) vs. top-down (anthropogenic effect via fisheries, for ex., Lehodey et al. 2009) are basically unresolved. A similar issue remains for the carbon cycle in terms of the role of the thermocline variability as a bottom up forcing or dynamical driver for air-sea CO_2 flux variability vs. the surface mixed layer variability or the thermodynamic driver for pCO_2 and air-sea exchanges of CO_2. Anthropogenic CO_2 forcing is clearly confounded in this case with the global warming impact on the circulation itself and we will not attempt here to untangle the direct and indirect anthropogenic forcing of CO_2 variability.

This line of analysis will help the assessment of the total carbon budget and its interannual-to-decadal variability which is a focus of the Regional Carbon Cycle and Assessment Processes (RECCAP), which focuses on quantifying the interannual variability of regional carbon fluxes over land and the oceans where partitioning into different regions is accomplished by the prior knowledge about the expected CO_2 flux variability. Therefore our study should offer highly relevant insights into regional specificities of interannual variability related to climate mode anomalies that should be targeted.

BGD
8, 4239–4280, 2011

The following is the structure of the remaining parts of this paper. In Sect. 2 we describe the data and methods used. In Sect. 3 we propose a regional structure of North Pacific air-sea CO_2 fluxes in response to the PDO through correlation, partial correlation and singular value decomposition analyses. The results are discussed and concluding thoughts are offered in Sect. 4.

2 Data and methods

In this study we mainly use an optimized estimate of the air-sea CO_2 flux for 25 yr spanning the period 1980–2004, based on a model with data assimilation which is derived from the work of Valsala and Maksyutov (2010, hereinafter referred to as OTTM). The total span of assimilation involved in OTTM is from 1996 to 2004. Prior to this period, interannual anomalies from the forward model are added to the seasonal climatology from the assimilation period of 1996–2004. In addition to this product, we also use air-sea CO_2 fluxes from two independent sources for comparison purpose and they are taken from McKinley et al. (2004a), spanning 1980–1999 and Le Quéré et al. (2005), over 1980–2004. These two products are from simulations of BGCMs. In addition to the model based estimates, we also use a pCO_2 field reconstructed for the North Pacific using a neural network approach developed by Telszewski et al. (2011). This dataset covers only the period from 2002 to 2008.

The model details and the method of CO_2 flux estimations are described in their respective papers and therefore only a brief summary for each data set is provided here. The optimized air-sea CO_2 fluxes of OTTM represent a variational assimilation of surface ocean pCO_2 observations into a relatively simple biogeochemical model. This model comprises of an offline tracer transport model and a phosphate dependent ecosystem model based on McKinley et al. (2004a). A variational assimilation is used to constrain the surface ocean model pCO_2 using corresponding ship track observations from the database of Takahashi et al. (2007). The seasonal to interannual pCO_2 are assimilated by applying separate weights based on the model interannual variance.

BGD
8, 4239–4280, 2011

The details of the assimilation, error estimates and comparison with observational climatology of Takahashi et al. (2009) can be found in Valsala and Maksyutov (2010).

The second model output used here is taken from the forward simulations of McKinley et al. (2004a). This is also an offline model run with MITgcm circulations and a phosphate dependent ecosystem model. This model comprises of three biogeochemical tracers and they are dissolved inorganic carbon (DIC), phosphate and oxygen. The CO_2 fluxes from this model offer a reasonable comparison with the annual mean air-sea CO_2 fluxes compiled by Takahashi et al. (2009). This data is also used in McKinley et al. (2006). The third model product we used is from Le Quéré et al. (2005) where a 24-component ecosystem is run with a state-of-the-art general circulation model (see also Buitenhuis et al., 2006 for details).

The fourth pCO_2 field used in our analysis was derived using an artificial neural network, a statistical method recently adapted for the spatial and temporal interpolation of the available measurements of marine pCO_2. The Self Organizing Map (SOM) was shown to allow a near-real time monitoring of the basin-wide, multi-year marine pCO_2 field by combining in-situ pCO_2 measurements, satellite data and operational ocean models (Telszewski et al., 2009). The SOM results used in this study benefit from several technical improvements as well as major changes of the calculating system (Telszewski et al., 2011). The authors hypothesize that seawater pCO_2 in the North Pacific may be parameterized as a function of basin-wide available parameters: sea surface temperature, mixed layer depth, chlorophyll-a concentrations, sea surface height anomalies and sea surface salinity. The SOM's ability to extract numerous relationships between input parameters simultaneously, despite the spatial and temporal sparseness of pCO_2 measurements allows for a truly basin-wide, data-based analysis of the pCO_2 field over several years.

BGD
8, 4239–4280, 2011

3 Results

Four independent products of CO_2 and pCO_2 described above are used in this study to mainly seek as robust a conclusion as possible on the climate-carbon connections in the North Pacific. Once a consistent regional and temporal variability of North Pacific CO_2 fluxes are obtained, we perform extended analysis on the optimized estimate of CO_2 flux data of OTTM. We begin our analysis by examining the robustness of our optimized air-sea CO_2 fluxes in the North Pacific in terms of its interannual variability compared to the seasonal cycle. The pCO_2 residual errors and error reductions of this optimized data are documented in Valsala and Maksyutov (2010). Here we present results from an extended analysis of the interannual and decadal variability.

The offline model employed in the construction of OTTM fluxes is driven by monthly re-analysis input of ocean currents and other parameters such as temperature and salinity. The only sub-monthly variability present in their model was in the wind speed data used in the calculation of air-sea CO_2 fluxes. However, the model assimilates ship track pCO_2 whenever observations are available. Considering the rather coarse resolution ($1^\circ \times 1^\circ$) of the model, it may suffer from representativity errors (RE) while incorporating the high-frequency sampling of ship track data through assimilation. In order to verify the model RE and the signal preserved in the data on seasonal-to-interannual time scales, we performed a signal to noise Ratio (SNR) analysis following a simple method derived from Ballabrera-Poy et al. (2003).

3.1 Analysis of the signal to noise ratio of air-sea CO_2 fluxes

The SNR analysis of OTTM air-sea CO_2 flux is carried out as follows. The time series of CO_2 flux c at each grid point is separated into components of seasonal, c^s, and interannual, c^a, time scales, and noise ε. The seasonal component is calculated by fitting annual and semi-annual harmonics to the total flux c. The interannual component, c^a, is found by subtracting c^s from c. This, however, will result in a combination of true c^a and ε. A harmonic filtering is then applied for cycles of above the annual period and

BGD
8, 4239–4280, 2011

are subtracted out. The residual is taken as the noise, ε. The interannual SNR is calculated as $\sigma_a^2/\sigma_\varepsilon^2$ and total SNR is calculated as $(\sigma_a^2+\sigma_s^2)/\sigma_\varepsilon^2$; where σ^2 represents the variances of interannual, seasonal and noise components (see Ballabrera-Poy et al., 2003 for further details). The interannual and total SNR are shown in Fig. 1. The interannual SNR is weaker than the seasonal SNR by an order of magnitude. The subarctic and northern part of the subtropical North Pacific has interannual SNR values below 1 (shaded white). The subtropical and the tropical regions have SNR above 1 and at places values exceeding 3 to 4. The seasonal cycle of the air-sea CO_2 flux also dominates in the North Pacific over the interannual variability. This is consistent with the findings of McKinley et al. (2006) who reported that the counteracting influences of SST, DIC and alkalinity on pCO_2 cause a weak pCO_2 interannual variability. The interannual variance (see Fig. 1d) is stronger to the east of Japan over the Kuroshio and Oyashio confluence zone. The inverse of this interannual variability is used as a weight to limit the seasonal cycle constraints imposed during assimilation, i.e, the model is allowed to evolve freely in regions where the interannual signals were stronger unless ship track data were available at those locations.

The seasonal variance of air-sea CO_2 fluxes on annual and semi-annual cycles is stronger in the subarctic North Pacific (Fig. 1e). At the northeastern subtropical Pacific, on the other hand, the seasonal variance is weaker. The error variances are mostly located along Kuril and Aleutian Island chains, perhaps indicating that the wind driven coastal upwelling creates high frequency variability (Fig. 1f) . It should be also noted that the ship track pCO_2 during 1996 to 1998 were sampled through these routes (Zeng et al., 2002). Therefore the relatively high error variance in this part may be originating from the model's inability to represent high-frequency variability in the pCO_2 data during the assimilation.

The SNR analysis suggests that the seasonal cycle in the North Pacific CO_2 fluxes is much stronger than the interannual signal. This is consistent with the findings of McKinley et al. (2006). The interannual variability captured in our estimates should be analyzed in conjunction with the SNR map and should consider only variability in

BGD
8, 4239–4280, 2011

regions where SNR has a value above 1. We will use this as a guidance to assess the interannual variability of the North Pacific CO_2 fluxes retrieved from the subsequent data analysis.

Figure 2 represents the annual mean air-sea CO_2 flux from assimilation as well as from observations of Takahashi et al. (2009). The bottom panel shows the seasonal correlation between assimilation and observations, and they are above 99% significance level in most parts, with some poor correlation points at grid levels along the island chains of Kuril and Aleutian, where we observe somewhat higher error variances in the assimilation. Except some differences in seasonal cycle at a few grid points, the overall North Pacific CO_2 flux from assimilation has a remarkably high correlation with the observations. Valsala and Maksyutov (2010; their Figs. 13 and 14) compared the seasonal as well as interannual variability of air-sea CO_2 flux from this region with data from other sources.

3.2 Correlation between North Pacific CO_2 flux and PDO

The PDO is a decadal mode of climate variability in the North Pacific sector associated with changes in the strength of wintertime Aleutian Low (Trenberth and Hurrell, 1994, also see Schneider et al., 2005 for other contributors to PDO). The accompanying changes in the Ekman flow, surface ocean mixing and heat fluxes create corresponding anomalies in the ocean. The PDO is defined as the dominant pattern of SST variability in the North Pacific (Mantua et al., 1997). PDO goes through warm and cool phases of the cycle with each phase typically lasting about 20–30 yr. The causes of this phase swings are currently unknown and the mechanisms or the independence of PDO as a climate mode are also debated (e.g., Rodgers et al., 2004; Newman et al., 2003). The recent decades have seen a cool phase starting around 1945 switching to a warm phase in 1977. The warm phase continued until late 2008 with some short cold spells in the PDO index (see http://jisao.washington.edu/pdo/ for an up-to-date report). The warm epochs of PDO are associated with enhanced coastal ocean biological production in the Alaska sector and with inhibited productivity off the west coast of the United

BGD
8, 4239–4280, 2011

States, while cold PDO episodes tend to produce the opposite north–south pattern of marine ecosystem productivity (Mantua et al., 1997).

In order to identify the spatial patterns of the North Pacific CO_2 flux variability with respect to PDO, we start with a simple correlation analysis. The CO_2 fluxes are deseasonalized and detrended before calculating the correlations. Figure 3 illustrates the point-to-point correlation between monthly air-sea CO_2 flux anomalies and PDO index for three flux products, viz., (left) OTTM and forward models of (middle) McKinley et al. (2004a) and (right) Le Quéré et al. (2005). The correlations are found from 300 monthly values between 1980 and 2004 in the OTTM data set and Le Quéré et al. (2005) with corresponding monthly index of PDO. In the case of McKinley et al. (2004a), only 240 months are used from 1980 to 1999. All the correlations shown above are significant at levels of 90% or above in two-tailed t-test. A careful examination of the correlation patterns suggest that PDO organizes regional responses in the air-sea CO_2 flux anomalies of the North Pacific. Considering both the clustering of correlations and the SNR of the interannual signal (see Fig. 1), we categorized four boxes of positive and negative correlations. The positive correlation boxes are located in the northwest and southeast part of the domain. Other two boxes of negative correlations are oriented in the northeast and southwest direction of the domain. It can be seen from Fig. 1a that the interannual SNR are reasonably large in the southern boxes, whereas they are relatively weak but statistically significant in the northern boxes. We discarded the correlations on the subarctic North Pacific from the boxes because their interannual SNR is below 1.

A similar analysis of the other two flux estimates (column 2 and 3 of Fig. 3) shows that such regional structures are quite consistent among different CO_2 products. However slight re-orientation of boxes is required when we move from one data product to another, which is not unexpected because they are generated by entirely different sets of models with additional differences in resolutions and surface forcing.

Looking at the clustering of correlations in individual boxes, we defined an index of CO_2 flux in response to PDO (hereafter CO_2g_PDO) as the sum of area integrated

BGD
8, 4239–4280, 2011

CO_2 anomalies from two "red" boxes minus the corresponding sum over the two "blue" boxes. The index is shown in the bottom panel of Fig. 3 for each product as the black line. The PDO index is overlaid as a red line. Both lines are smoothed with a 12-month running mean. The CO_2g_PDO and PDO are correlated at above 95% significance level, especially because the regions for calculating CO_2g_PDO are chosen from areas where the correlations with PDO are significantly high. Therefore the interannual-to-decadal CO_2 flux anomalies in the North Pacific are clearly and fairly intimately related to PDO in the region represented by the four boxes shown in these figures.

Air-sea CO_2 flux is driven by the difference in pCO_2 between the ocean and the atmosphere as well as the piston velocity which is usually parameterized with wind speeds (e.g., Wanninkhof, 1992). In order to see what controls the CO_2 flux variability linked to PDO, we repeated the correlation analysis with the optimized OTTM pCO_2. The results are shown in Fig. 4. It can be seen that similar regional structures of correlations between pCO_2 and PDO exist similar as in the case of CO_2 fluxes. Therefore, the air-sea CO_2 flux anomalies linked to PDO as seen in the previous analysis are mainly driven by the pCO_2 anomalies. The index representing the pCO_2_PDO also correlated with PDO index at a significance level above 95%. Since seawater pCO_2 is controlled by both solubility and biological pumps. The biological pump relies to a large extent on the vertical supply of nutrients (horizontal advection can also be important), we expect that ocean dynamics, i.e., thermocline movements and mixed layer entrainment are crucial. The solubility pump on the other hand is more closely related to the thermodynamics, i.e., SST variability. An additional characteristic of this region is that the so-called transition zone chlorophyll front (TZCF) traverses this entire domain and demarcates the subtropical-subpolar boundary with a clear and significant impact on not only the dynamics and the thermodynamics of our domain but also the ecosystem and the biogeochemistry of all the boxes being studied here (Polovina et al., 2001). Detailed analysis of the interactions between the TZCF, PDO, and the correlations being discussed here is beyond the scope of the present study.

BGD
8, 4239–4280, 2011

Figure 5 shows a similar analysis repeated with pCO_2 derived from neural network algorithm provided by Telszewski et al. (2011) (see Sect. 2) but only for a relatively short period of time, between 2002 and 2008, therefore they are shown separately. The spatial features revealed from the neural network data show quite consistent patterns of regional dependency of pCO_2 and PDO over the boxes being considered, with some inter-box differences. For example the component of positive correlation from the northwestern box protruded into the northeastern box in the analysis of neural network pCO_2 data. On the whole the regional relationship between pCO_2 and PDO at interannual time-scale is also maintained when the shorter period of time is considered. The pCO_2_PDO index correlates with the PDO index in this case as well (Fig. 5, bottom panel). The northeast corner of the domain, i.e., the Gulf of Alaska displays significant differences between the longer and the shorter time-series which is likely related to the biennial ENSOs of 2002, 2004, and 2006, dominating the teleconnections over this region which will be analyzed and reported elsewhere.

3.3 Interannual and interdecadal relations of CO_2 fluxes and PDO

There is considerable uncertainty, however, about whether the PDO is truly independent of the leading mode of tropical variability, i.e. ENSO (Rodgers et al., 2004; Newman et al., 2003). The spatial patterns of interannual SST variability in the Pacific Ocean show a pronounced maximum in the tropical east Pacific and weaker center of opposite sign in the central North Pacific. While on decadal timescales, the relative strength of these centers is reversed (Zhang et al., 1997). The simultaneous correlations of ENSO index and PDO are relatively weak especially during winter months (Mantua et al., 1997).

It is evident from the CO_2g_PDO index shown in Fig. 3 that the index has both a low-frequency (i.e. a decadal time scale) and a high-frequency (interannual) component. Therefore it is reasonable to expect that the individual correlations between decadal and interannual variability of CO_2 flux are linked to PDO. Here "decadal" is not intended to represent a 20–30 yr cycle at which the PDO typically switches between cold and

BGD
8, 4239–4280, 2011

warm phases. But the focus is on periods longer than ENSO and in the range of 10–15 yr.

In order to show separate correlations of CO_2g_PDO index on these two time scales, we isolated the decadal component of CO_2 flux variability using the harmonic filter analysis. The variability of 6.5 yr and above was filtered out from the interannual anomalies of CO_2 flux and correlations with correspondingly filtered PDO index are computed. Figure 6 illustrates that the correlation found both at decadal and on interannual time-scales are almost identical albeit with some differences in the intra-box correlation features. For example, the northwestern box is consistent between the two cases (see Fig. 6a,b). However, there are differences in correlations over the northeast box between the interannual and decadal time-scales. On decadal scale, there is some positive correlation extending into the northeastern box. On the other hand the correlations are stronger in the southeast box in the decadal case than the corresponding correlations for the interannual case. The southwest box shows a stronger decadal than interannual signal. The bottom panels show the CO_2g_PDO and PDO indices at both decadal and interannual time-scales. Both correlate at significance levels above 95%. This analysis allows us to conclude that the correlations between CO_2 fluxes in the North Pacific and the climate drivers are significant both at low and high frequencies.

It is a general practice to discuss the North Pacific variability as a seasonal average variability only during the winter months because of the weak correlations between the winter time PDO and ENSO (Mantua et al., 1997). We calculated the correlations of winter PDO with corresponding winter CO_2 flux anomalies. The months from November to March are used to represent the winter-PDO, and the CO_2 flux anomalies of corresponding months are also averaged to determine the correlations. Similarly summer months of June and July are used for summer-PDO and CO_2 flux correlations. Figure 7 shows that the winter-PDO explains a four-box structure in the correlation with the same polarity as was seen in the previous sections. On the other hand, during summer months this four box polarity is lost and the North Pacific CO_2 flux is largely negatively correlated with the summer-PDO with some positive correlation only in the

BGD
8, 4239–4280, 2011

southeast box. This analysis shows that the winter time PDO is essentially responsible for producing a four-box structure in the North Pacific CO_2 fluxes with positive polarity in the northwest and the southeast boxes and with opposite polarity in the other two boxes. This again confirms that such a distribution of the North Pacific air-sea CO_2 fluxes is driven by the PDO because the signal is stronger during winter months when the "grip" of ENSO on PDO is weaker. The subpolar-subtropical-tropical interactions have seasonal variations which affect the seasonal vulnerability of our study region to climate modes (see for example, Vimont, 2005). The seasonal aspects of this are also important since the subtropical anticyclone itself undergoes a significant weakening during the winter and the subpolar low expands to reach into the tropics (Nigam and Chan, 2009). The dynamical and thermodynamical responses of these changes on CO_2-flux variability will need further detailed analysis which is beyond the scope of this study.

In order to provide additional support for individual effects of PDO and ENSO on the correlations with CO_2 fluxes, we performed a "partial correlation" analysis. In case of a set of three variables which show mutual correlations, the partial correlation analysis attempts to remove the effect of one component over the other two (Ashok et al., 2007). Figure 8 shows the correlations between monthly PDO index and CO_2 flux anomalies after removing the effect of ENSO through partial correlation analysis. The four-box structure with diagonal polarities is still maintained in this case confirming the PDO as the dominant driver of the correlation features in the North Pacific air-sea CO_2 fluxes. Again, to untangle the dynamic and thermodynamic components of the CO_2 variability forcing, the persistence of PDO and its impacts on wind-speeds and wind-stress curls have to be analyzed together with ENSO impacts on the same. In hindsight, it is not surprising that PDO dominates the region, since ENSO is most directly teleconnected to the Aleutian low which occupies the northwest corner of our domain, whereas PDO signature affects all four boxes and persists over decadal time-scales. We use combined EOF analysis to extract some clues into the dynamic and thermodynamic contributions to CO_2 variability in the study domain.

BGD
8, 4239–4280, 2011

3.4 Component analysis of CO_2 fluxes with ocean-atmosphere variability

Although the correlation analysis presented above identifies the spatial and temporal structures of the North Pacific CO_2 flux variability with respect to PDO, it does not, by itself, offer any mechanistic insights. We carried out a component analysis of pCO_2 in terms of SST, DIC, Alkalinity and Salinity and performed the correlations with each of them. These components are obtained by a method similar to that described in McKinley et al. (2006). Our results are similar to the findings of McKinley et al. (2006) in that the partial changes of pCO_2 due to SST, DIC and Alkalinity are similar in magnitude and opposite in phase. Thus the net change in pCO_2 is the sum of the partial changes of these factors, and the residual of the sum is the interannual variability. In our study, the correlation analysis only organizes this residual interannual variability in a certain regional pattern. Considering the robustness of correlation patterns between the four data products examined here, it seems reasonable to assume that their existence is not purely by chance.

In this section, we examine the combined variability of air-sea CO_2 fluxes in terms of a few oceanic and atmospheric variables in order to see their covariability with PDO. We employed a combined empirical orthogonal function (CEOF) analysis between these pre-selected variables. CEOFs capture the joint variability of two variables in space and time. If such variability exists in the case of North Pacific CO_2 fluxes and if they correlate with PDO, it should provide a basis for the existence of the spatial structure and point to the mechanism responsible for the structure of interannual CO_2 flux variability.

We begin the analysis by calculating the CEOFs between the anomalies of CO_2 fluxes and SST over the domain under consideration. The CEOFs of detrended, deseasonalized CO_2 flux and SST anomalies were calculated. The data are passed through a 12-month running mean before computing the CEOF. The SST anomaly was taken from Simple Ocean Data Assimilation prepared by Carton and Giese (2008). The top-panel of Fig. 9 shows the CEOF-1 of CO_2 flux over SST anomaly. The middle-panel shows the CEOF-1 of SST over CO_2 flux anomaly. And the bottom panel shows the

BGD
8, 4239–4280, 2011

principle components (PC) of the dominant mode. The red line in the bottom panel shows the PDO index. All the spatial patterns (i.e. CEOFs) are multiplied with standard deviations of respective variables. Therefore they have meaningful units. All PCs are normalized with respective standard deviations in order to non-dimensionalize them.

The CEOF extracts the response of CO_2 related to SST and their PC-1 shows a clear correlation with PDO (above 95% level). Therefore, the dominant mode of SST variability in the North Pacific does have an influence on defining the dominant mode variability in the CO_2 flux and both are controlled by PDO. This is clear evidence that the North Pacific CO_2 fluxes do respond to PDO. The CEOF-1 of SST combined with CO_2 flux shows a typical PDO signature in SST during a warm phase as shown in Mantua et al. (1997). The corresponding CO_2 flux responses show a sink in the subtropical gyre where the SST anomalies are found to be negative. This shows a direct relation between pCO_2 and SSTs, i.e., a reduced pCO_2 during a cold SST anomaly. In the northern subtropical to subarctic North Pacific, the CO_2 flux maybe expected to show a positive anomaly in response to the warm anomaly in the SST. However, there are negative anomalies of CO_2 flux at few spots corresponding to positive SST anomalies. This is likely a combination of the noise in the model (SNR in this region is significantly low; see Fig. 1) and the dynamic component of the CO_2 flux variability (see discussion below). In fact the Aleutian low and the Kuroshio add significant dynamic component to the flux variability. The variance explained by CEOF-1 is 18%.

We calculated the CEOF of CO_2 flux and wind stress anomalies. We choose the wind stress in this analysis because it offers a squared wind relation with the CO_2 flux, which corresponds to the squared wind speed and variance used in the CO_2 exchange calculation. The results are shown in Fig. 10. The top-panel shows the CEOF-1 of CO_2 flux and wind stresses, which is very similar to the CEOF-1 of CO_2 flux and SST (cf. Fig. 9). Wind stresses (vectors) show the dominant mode of wind pattern corresponding to the warm phase of PDO (Mantua et al., 1997). The middle panel shows the CEOF-1 of SST and wind vectors from CEOF with CO_2. This panel shows a clear PDO type SST-wind relationship as can be expected because of the dominance of PDO

BGD
8, 4239–4280, 2011

forcing. The bottom-panel shows the PC-1 of CO_2 with wind stresses (black line) and PDO index (red line). The variance explained is 20%. The PC shows that the North Pacific CO_2 sink increases when the zonal winds associated with the PDO strengthen. This can be seen from the CEOF-1 pattern of CO_2 and wind stress components in the top-panel of Fig. 10. Both PCs (Figs. 9 and 10) correlate with PDO above 95% significance level.

The CEOF analysis was also done between CO_2 fluxes and sea surface height (SSH) anomalies. The concomitant analysis of CEOFs of CO_2 and SSH as well as CO_2 and SST provides insights into the dominant mechanisms of CO_2 interannual variability in terms of dynamic and thermodynamic contributions. Figure 11 shows CEOF analysis of CO_2 and SSH anomalies. The top-panel of the figure shows that the interannual variability of CO_2 has a similar structure in SSH as that found in SST and wind stresses. This co-variability of CO_2 fluxes with SSH, SST and wind anomalies show their strong mutual coupling through dynamics and thermodynamics. For example, the subtropical gyre shows a CO_2 sink in the CEOFs of CO_2 with SST and SSH. This leads to the conclusion that there is a dominant thermodynamic control on CO_2 fluxes in the subtropical gyre. For example, a cold SST anomaly leads to a sink of CO_2 through enhanced solubility. On the other hand, the shoaling of thermocline in the subtropical gyre and the increase in surface DIC has no net influence on CO_2 fluxes since it is counteracted by increased solubility and a relatively small increase in CO_2 flux. The role of the dynamics is thus muted by the thermodynamics. It is worth mentioning that the seasonal cycle of CO_2 fluxes in the North Pacific is nearly an order of magnitude larger than the corresponding interannual variability. The seasonal cycle of CO_2 flux is strongly influenced by the thermodynamics of the mixed layer, and slight changes in the seasonality from year to year drive interannual variability of CO_2 fluxes in the subtropical gyre of the North Pacific.

BGD
8, 4239–4280, 2011

The thermodynamic control on CO_2 fluxes, however, appears to be weaker in the subarctic North Pacific. This is elicited by examining the top-panels of Figs. 9–11. These three panels show that there are marked differences in the CO_2 flux variability explained by SST, wind and SSH. In order to see what causes the regional clustering of correlations of CO_2 fluxes with PDO (see Sect. 3.1), we carried the combined CEOF analysis of CO_2 flux, SST and SSH together and results are shown in Fig. 12. The combined variability of SST and SSH (or can be rightfully interpreted as variability of thermodynamics and dynamics, respectively) causes a tentative four-box shape in the CEOF of CO_2 flux (top-panel of Fig. 12). For the purpose of comparison, the regional clustering of correlations as explored in Sect. 3.1 is repeated in the middle panel of the figure. This panel suggests that the combined influence of dynamics and thermodynamics can cause such regional homogeneity of CO_2 flux variability in response to the PDO. The bottom panel of the figure shows the PC-1 of CEOF, the CO_2g_PDO and PDO indexes. They all correlate with each other above a 95% significant level.

The spatial and temporal correlations between CEOF-2 of CO_2 and other variables described above in the CEOF analysis were also similar and significant. This is consistent with the findings of McKinley et al. (2006) in that the first two EOFs show significant correlations with PDO. However the relation and independence of EOF-1 and 2 type interannual variability between PDO and ENSO have been discussed in several previous studies and a clear conclusion is not available yet (Lorenzo et al., 2008; Latif and Barnett, 1996). Therefore, we restrict our analysis to the first modes of EOFs.

4 Discussion and conclusion

Several features of the interannual variability of air-sea CO_2 flux linked to PDO are isolated in this study. The results lead to interesting discussions in terms of assessing the trends in the surface ocean pCO_2. Our analysis puts forward a recommendation that we should take into account the natural variability while assessing the secular trends in the pCO_2 of the North Pacific, especially when they are found with short term

BGD
8, 4239–4280, 2011

observations. Our analysis suggests that such trends could be a part of the larger interannual to decadal variability.

Although the correlative as well as CEOF analyses identified a spatial structure of CO_2 flux variability with the PDO, the magnitude of the anomalies is relatively small. This can be expected in the case of North Pacific CO_2 fluxes because it has weak interannual anomalies. We regressed the PDO index against CO_2 fluxes over the four-boxes depicted in the above analysis and found that the net variability is a sink of $0.015\,Pg\,C\,yr^{-1}$ (Fig. 13). In the figure, the regressed anomalies are shown only where the SNRs of interannual variability are above one. It is interesting that a positive PDO causes a net air to sea flux in the North Pacific. The annual mean sink of CO_2 in the domain under consideration is, however, nearly $0.35\,Pg\,C\,yr^{-1}$. The internal variability and the inability to extract the internal variability from limited data appear to be a major impediment to robust conclusions about the source/sink variability in the domain. Thus, estimating the SNR as best as we can becomes critical.

The analysis presented here used four independent CO_2 products and attempted to extract the most robust features in the regional responses of air-sea CO_2 fluxes in the North Pacific to climate anomalies. In addition to the surface fluxes, we also extended the analysis to the ocean interior in order to retrieve deep structures of interannual variability as visible in the model outputs of DIC. Our analysis revealed that the sub-surface DIC also responds to the thermocline movements induced by the PDO forcing. For example, Fig. 14 depicts the correlation coefficients between model DIC and PDO index (top-panel) at the surface level and (middle-panel) at a 100 m depth level. The overlaid contours are that of CEOF-1 of SST over CO_2. The cold SST anomaly reflects an increase in DIC both in the surface as well as at 100m depth, which indicates a shoaling of thermocline and subsequent increase in DIC (see also McKinley et al., 2006). However, it is likely that such an increase in DIC is ineffective in driving CO_2 flux responses which appear to be mostly controlled by the SST cooling, especially in the subtropical gyre of the North Pacific. This is confirmed by the CO_2 flux anomalies in the subtropical gyre which show a sink (top-panels; Figs. 9–11) indicating an active

BGD
8, 4239–4280, 2011

response of CO_2 fluxes to the cold SST anomalies associated with the PDO (middle-panel; Figs. 9 and 11). This leads to the conclusion that the thermodynamics (i.e. SST and CO_2 flux relationships) plays a dominant role in the subtropical Pacific.

Figure 14 also shows a vertical propagation of the PDO signal. The signal is illustrated as vertical section of correlation coefficients between DIC and PDO, averaged zonally over 140° E to 140° W. The correlations extend to the thermocline in the subtropical region (nearly 100 m) which is within the reach of seasonal mixed layer, whereas they extend to a depth greater than 300 m in the subarctic region. The seasonal amplitude of mixed layer depth (winter maximum minus summer minimum) in the subtropical region is ~ 100 m (with annual mean mixed layer depth of 110 m) whereas in the subarctic region it is ~ 50 m (with annual mean mixed layer depth of 90 m). The extent of vertical propagation of PDO signal in the subtropical region shows that the seasonal cycle of vertical mixing carries the PDO induced surface changes to the thermocline, again ensuring that the thermodynamic cycle could be the dominant mechanism of air-sea CO_2 fluxes in that region. In contrast, the vertical propagation of the PDO signal in the subarctic is much deeper even with the shallow seasonal amplitude of the mixed layer depth of only 50 m. Therefore, one may assume a role of dynamical changes in thermocline depths may be significant in this region. This is consistent with the CEOFs between CO_2 and SSH as well as between CO_2 and SST in the subarctic region. The SSH induced deepening of thermocline and negative CO_2 flux anomalies were noted especially in the eastern subarctic gyre (see Fig. 11).

In our analysis, as well as in McKinley et al. (2006) it is reflected that the individual components that control the surface ocean pCO_2 in the North Pacific respond to PDO with significant amplitudes, whereas their combined effects make a net change which is feeble in amplitude, and scattered in space. Despite this general agreement, our study suggests that, within the scattered spatial correlations of CO_2 flux anomalies with PDO, there seem to be regional clustering of positive and negative correlations, and we propose that they are organized into four distinct regional boxes. This hypothesis was tested with four different CO_2 products, and a general conclusion is reached. The

BGD
8, 4239–4280, 2011

implication of our results is that the assessment of pCO_2 trends in terms of surface ocean pCO_2 should consider the natural variability and its regional patterns.

The conclusions of this study are restated here. (1) The North Pacific air-sea CO_2 fluxes show significant regional correlations with the PDO and they are oriented along two positive polarity boxes in the northwest–southeast directions and two negative polarity boxes in the northeast–southwest direction. (2) The combined and individual effects of ENSO and PDO on the regional clustering of correlations were identified and it is shown that PDO is the dominant cause for such regional correlations. (3) The combined EOF analyses were carried out between CO_2 fluxes and few key variables of air-sea interactions and it was found that in the subtropical North Pacific, the air-sea CO_2 fluxes are generally controlled by the thermodynamics (i.e. vertical mixing, seasonal cycle of SST and CO_2 fluxes), whereas, in the subarctic North Pacific, there could be a dominance of dynamically induced controls on the CO_2 fluxes (i.e. wind induced thermocline heaving, surface DIC convergence and CO_2 fluxes). However, we note that the last point is only suggested by our study and it requires more model simulations and diagnostics as well as ecosystem assessments in order to fully reveal the controls of thermodynamics and dynamics in the interannual variability of air-sea CO_2 fluxes in the North Pacific. That is left as a future study and will be reported elsewhere. To the extent that climate change is expected to manifest into changes in ENSO and PDO, the climatic impacts on the carbon cycle are also expected to occur through these dynamic-thermodynamic processes in addition to ecosystem responses. Our study will hopefully provide a framework to assess the response of the air-sea exchanges of CO_2 and the oceanic carbon cycle to climate change.

Acknowledgement. This work was carried out as part of the GOSAT carbon cycle research project at CGER, NIES. Computational resources were provided by the supercomputer facility at NIES. M. T. acknowledges the use of the High Performance Computing Cluster supported by the Research Computing Service at the University of East Anglia, Norwich, UK. M. T., S. N. and Y. N. were kindly supported by Global Environmental Research Account for National Institutes from Ministry of Environment, Japan. R. M. gratefully acknowledges the generous support by the Divecha Climate Center and the hospitality of CAOS at IISc, Bangalore.

BGD
8, 4239–4280, 2011

References

Ashok, K., Nakamura, H., and Yamagata, T.: Impacts of ENSO on the Southern Hemisphere storm-track activity during Austral winter, J. Climate, 20, 3147–3163, 2007.

Baker, D. F., Doney, S. C., and Schimel, D. S.: Variational data assimilation for atmospheric CO_2, Tellus B, 58, 359–365, 2006.

Ballabrera-Poy, J., Murtugudde, R., and Christian, J. R.: Signal-to-noise ratio of observed monthly tropical ocean color, Geophys. Res. Lett., 30, 1645, doi:10.1029/2003GL016995, 2003.

Buitenhuis, E., Le Quéré, C., Aumont, O., Beaugrand, G., Bunker, A., Hirst, A., Ikeda, T., O'Brien, T., Piontkovski, S., and Straile, D.: Biogeochemical fluxes through mesozooplankton, Global Biogeochem. Cy., 20, GB2003, doi:10.1029/2005GB002511, 2006.

Carton, J. A. and Giese, B.: A reanalysis of ocean climate using Simple Ocean Data Assimilation (SODA). Mon. Weather Rev., 136, 2999–3017, 2008.

Chavez, F. P., Pennington, T. J., Castro, C. G., Ryan, J., Michisaki, R. P., Schlining, B., Walz, P., Buck, K., McFadyen, A., and Collins, C. A.: Biological and chemical consequences of the 1997–1998 El Niño in central California waters, Prog. Oceanogr., 54, 205–232, 2002.

Di Lorenzo, E., Schneider, N., Cobb, K. M., Franks, P. J. S., Chhak, K., Miller, A. J., McWilliams, J. C., Bograd, S. J., Arango, H., Curchitser, E., Powell, T. M., and Riviere, P.: North Pacific Gyre Oscillation links ocean climate and ecosystem change, Geophys. Res. Lett., 35, L08607, doi:10.1029/2007GL032838, 2008.

Feely, R., Boutin, J., Cosca, E. C., Dandonneau, Y., Etcheto, J., Inoue, H., Ishii, M., Le Quéré, C., Mackey, D., and McPhaden, M.: Seasonal and interannual variability of CO_2 in the Equatorial Pacific, Deep-Sea Res., 14, 2443–2469, 2002.

Gruber, N., Gloor, M., Mikaloff Fletcher, S. E., Doney, S. C., Dutkiewicz, S., Follows, J. M., Gerber, M., Jacobson, A. R., Joos, F., Lindsay, K., Menemenlis, D., Mouchet, A., Müller, A. S., Sarmiento, J. L., and Takahashi, T.: Oceanic sources, sinks and transport of atmospheric CO_2, Global Biogeochem. Cy., 23, GB1005, doi:10.1029/2008GB003349, 2009.

Gurney, K. R., Law, R. M., Denning, A. S., Rayner, P. J., Pak, B., and Transom-3-L2-modelers: Transcom-3 inversion intercomparison: control results for the estimation of seasonal carbon sources and sinks, Global Biogeochem. Cy., 18, GB1010, doi:10.1029/2003GB002111, 2004.

BGD
8, 4239–4280, 2011

Hurrell, J. W.: Decadal trends in the North Atlantic oscillation regional temperatures and precipitation, Science, 269, 676–679, 1995.

Jones, D., Collins, M., Cox, P. M., and Spall, S. A.: The carbon cycle response to ENSO: A coupled climate carbon cycle model study, J. Climate, 14, 4113–4129, 2001.

Latif, M. and Barnett, T. P.: Decadal climate variability over the North Pacific and North America: Dynamics and predictability, J. Climate, 9, 2407–2423, 1996.

Le Quéré, C., Orr, J. C., Monfray, P., Aumont, O., and Madec, G.: Interannual variability of the oceanic sink of CO_2 from 1979 through 1997, Global Biogeochem. Cy., 14, 1247–1265, 2000.

Le Quéré, C., Harrison, S. P., Colin Prentice, I., Buitenhuis, E. T., Aumont, O., Bopp, L., Claustre, H., Cotrim Da Cunha, L., Geider, R., Giraud, X., Klaas, C., Kohfeld, K. E., Legendre, L., Manizza, M., Platt, T., Rivkin, R. B., Sathyendranath, S., Uitz, J., Watson, A. J., and Wolf-Gladrow, D.: Ecosystem dynamics based on plankton functional types for global ocean biogeochemistry models, Glob. Change Biol., 11, 2016–2040, 2005.

Le Quéré, C., Rödenbeck, C., Buitenhuis, E. T., Conway, T. J., Langenfelds, R., Gomez, A., Labuschagne, C., Ramonet, M., Nakazawa, T., Metzl, N., Gillett, N., and Heimann, M.: Saturation of the southern ocean CO_2 sinks due to recent climate change, Science, 316, 1735–1738, 2007.

Le Quéré C., Raupach, M. R., Canadell, J. G., Marland, G., Bopp, L., Ciais, P., Conway, T. J., Doney, S. C., Feely, R. A., Foster, P., Friedlingstein, P., Gurney, K., Houghton, R. A., House, J. I., Huntingford, C., Levy, P. E., Lomas, M. R., Majkut, J., Metzl, N., Ometto, J. P., Peters, G. P., Prentice, I. C., Randerson, J. T., Running, S. W., Sarmiento, J. L., Schuster, U., Sitch, S., Takahashi, T., Viovy, N., van der Werf, G. R., and Woodward, F. I.: Trends in the sources and sinks of carbon dioxide, Nat. Geosci., 2, 831–836, doi:10.1038/NGEO689, 2009.

Lehodey, P., Senina, I., Sibert, J., Bopp, L., Calmettes, B., Hampton, J., and Murtugudde, R.: Preliminary forecasts of Pacific bigeye tuna population trends under the A2 IPCC scenario, Prog. Oceanogr., 86, 302–315, 2010.

Lovenduski, N. S., Gruber, N., and Lima, C. D. I. D.: Enhanced CO_2 out gassing in the southern ocean from a positive phase of the Southern Annular Mode, Global Biogeochem. Cyc., 21, GB2026, doi:10.1029/2006GB002900, 2007.

Mantua, N. J., Hare, S. R., Zhang, Y., Wallace, J. M., and Francis, R.: A Pacific interdecadal climate oscillation with impacts on salmon production, B. Am. Meteor. Soc., 78, 1069–1079, 1997.

BGD
8, 4239–4280, 2011

McKinley, G. A., Follows, M. J., and Marshall, J.: Mechanism of air-sea CO_2 flux variability in the Equatorial Pacific and North Atlantic, Global Biogeochem. Cy., 18, GB2011, doi:10.1029/2003GB002179, 2004.

McKinley, G. A., Takahashi, T., Buitenhuis, E., Chai, F., Christian, J. R., Doney, S. C., Jiang, M.-S., Lindsay, K., Moore, J. K., Le Quéré, C., Lima, I., Murtugudde, R., Shi, L., and Wetzel, P.: North Pacific carbon cycle response to climate variability on seasonal to decadal timescales, J. Geophys. Res., 111, C07S06, doi:10.1029/2005JC003173, 2006.

Metzl, N., Brunet, C., Jabaud-Jan, A., Poission, A., and Schauer, B.: Summer and winter air-sea CO_2 fluxes in the Southern Ocean, Deep-Sea Res., 53, 1548–1563, 2006.

Newman, M., Compo, G. P., and Alexander, M. A.: ENSO-forced variability of the Pacific Decadal Oscillation, J. Climate, 23, 3853–3857, 2003.

Nigam, S. and Chan, S. C.: On the summertime strengthening of the Northern Hemisphere Pacific sea level pressure anticyclone, J. Climate, 22, 1174–1192, 2009.

Obata, A. and Kitamura, Y.: Interannual variability of the air-sea exchange of CO_2 from 1961 to 1998 simulated with a global ocean circulation-biogeochemistry model, J. Geophys. Res., 108, 3337, doi:10.1029/2001JC001088, 2003.

Park, G., Wanninkhof, R., Doney, S. C., Takahashi, T., Lee, K., Feely, R. A., Sabine, C. L., Trinanes, J., and Lima, I. D.: Variability of global net sea-air CO_2 fluxes over the last three decades using empirical relationships, Tellus B, 62, 352–368, 2010.

Patra, P. K., Maksyutov, S., Ishizawa, M., Nakazawa, T., Takahashi, T., and Ukita, J.: Inter-annual and decadal changes in the air-sea flux from atmospheric inverse modeling, Global Biogeochem. Cy., 19, GB4013, doi:10.1029/2004GB002257, 2005.

Polovina, J. J., Howell, E., Kobayashi, D. R., and Seki, M. P.: The transition zone chlorophyll front, a dynamic global feature defining migration and forage habitat for marine resources, Prog. Oceanogr., 49, 469–483, 2001.

Rödenbeck, C., Houweling, S., Gloor, M., and Heimann, M.: CO_2 flux history 1982–2001 inferred from atmospheric data using a global inversion of atmospheric transport, Atmos. Chem. Phys., 3, 1919–1964, doi:10.5194/acp-3-1919-2003, 2003.

Rodgers, K. B., Freiderichs, P., and Latif, M.: Tropical Pacific decadal variability and its relation to decadal modulations of ENSO, J. Climate, 17, 3761–3774, 2004.

Takahashi, T., Sutherland, S. C., and Kozyr, A.: Global ocean surface water partial pressure of CO_2 database: Measurements performed during 1968–2006 (Version 1.0). ornl/cdiac-152, ndp-08. Carbon Dioxide Information Analysis Center, 20 pp., 2007.

BGD

8, 4239–4280, 2011

Takahashi, T., Sutherland, S. C., Wanninkhof, R., Sweeney, C., Feely, R. A., Chipman, D. W., Hales, B., Friederich, G., Chavez, F., Sabine, C., Watson, A., Bakker, D. C. E., Schuster, U., Metzl, N., Yoshikawa-Inoue, H., Ishii, M., Midorikawa, T., Nojiri, Y., Kortzinger, A., Steinhoff, T., Hoppema, M., Olafsson, J., Arnarson, T. S., Tilbrook, B., Johannessen, T., Olsen, A., Bellerby, R., Wong, C. S., Delille, B., Bates, N. R., and de Baar, H. J. W.: Climatological mean and decadal changes in surface ocean pCO_2, and net sea-air CO_2 flux over the global oceans, Deep-Sea Res. Pt. II, 56, 554–577, 2009.

Telszewski, M., Chazottes, A., Schuster, U., Watson, A. J., Moulin, C., Bakker, D. C. E., González-Dávila, M., Johannessen, T., Körtzinger, A., Lüger, H., Olsen, A., Omar, A, Padin, X. A., Ríos, A., Steinhoff, T., Santana-Casiano, M., Wallace, D. W. R., and Wanninkhof, R.: Estimating the monthly pCO_2 distribution in the North Atlantic using a self-organizing neural network, Biogeosciences, 6, 1405–1421, doi:10.5194/bg-6-1405-2009, 2009.

Telszewski, M., Nojiri, Y., Usui, N., Nakaoka, S., and Miyazaki, C.: A neural network based estimates of the air-sea flux of CO_2 in the North Pacific: seasonal and interannual variability, in preparation, 2011.

Thomas, H., Prowe, A. E. F., Lima, I. D., Doney, S. C., Wanninkhof, R., Greatbatch, R. J., Schuster, U., and Corbière, A.: Changes in the North Atlantic oscillation influence CO_2 uptake in the North Atlantic over the past 2 decades, Global Biogeochem. Cy., 22, GB4027, doi:10.1029/2007GB003167, 2008.

Tjiputra, J. F., Polzin, D., and Winguth, A. E.: Assimilation of seasonal chlorophyll and nutrient data into an adjoint three-dimensional ocean carbon cycle model: sensitivity analysis and ecosystem parameter optimization, Global Biogeochem. Cy., 21, GB1001, doi:1029/2006GB002745, 2007.

Trenberth, K. and Hurrell, J.: Decadal atmosphere-ocean variations in the Pacific, Clim. Dynam., 9, 303–319, 1994.

Valsala, K. V. and Maksyutov, S.: Simulation and assimilation of global ocean pCO_2 and air-sea CO_2 fluxes using ship observations of surface ocean pCO_2 in a simplified biogeochemical offline model, Tellus B, 62(5), 821–840, doi:10.1111/j.1600-0889.2010.00495.x, 2010.

Vimont, D.: The contribution of interannual ENSO cycle to the spatial patterns of decadal ENSO like variability, J. Climate, 18, 2080–2092, 2005.

Wanninkhof, R.: Relationship between wind speed and gas exchange over the ocean, J. Geophys. Res., 97, 7373–7382, 1992.

BGD
8, 4239–4280, 2011

Zeng, J., Nojiri, Y., Murphy, P. P., Wong, C. S., and Fujinuma, Y.: A comparison of pCO_2 distributions in the Northern North Pacific using results from a commercial vessel in 1995–1999, Deep-Sea Res., 49, 5303–5315, 2002.

Zhang, Y., Wallace, J. M., and Battisti, D. S.: ENSO-like interdecadal variability in the Pacific, J. Climate, 10, 1004–1020, 1997.

BGD

8, 4239–4280, 2011

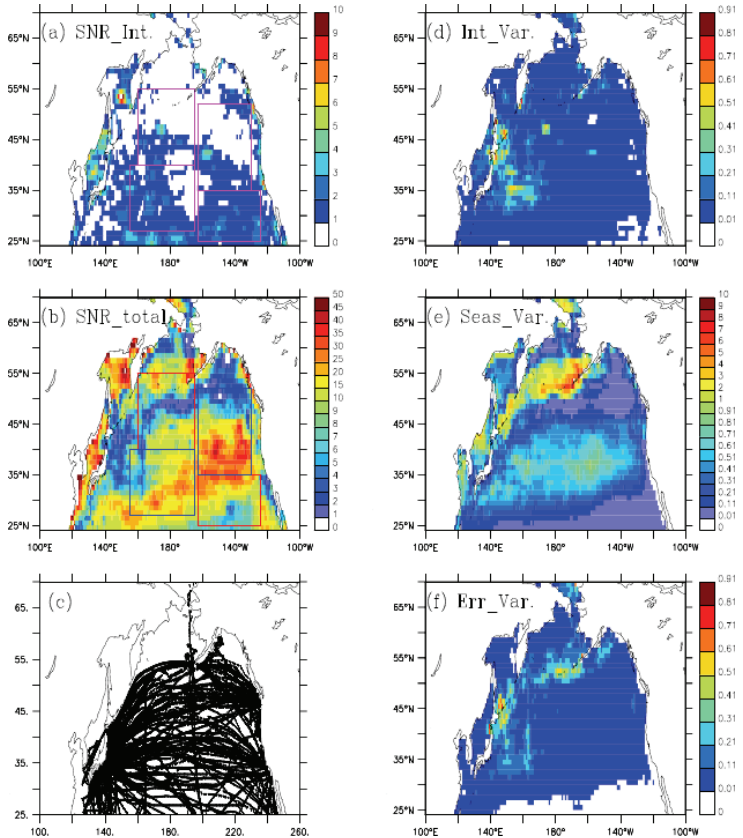

Fig. 1. The signal to noise ratio (SNR) of **(a)** interannual and **(b)** total air-sea CO_2 flux variability. **(c)** The total tracks of ship based pCO_2 used in the assimilation between 1996 and 2004. **(d)** Interannual, **(e)** seasonal and **(f)** error variances of air-sea CO_2 fluxes. Units of **(d–f)** are in $\times 10^{-14}\,(\mathrm{mol\,m^{-2}\,s^{-1}})^2$. Note that the color bar is different for each figure. SNR below 1 is shaded white. CO_2 flux data from assimilation are used.

BGD
8, 4239–4280, 2011

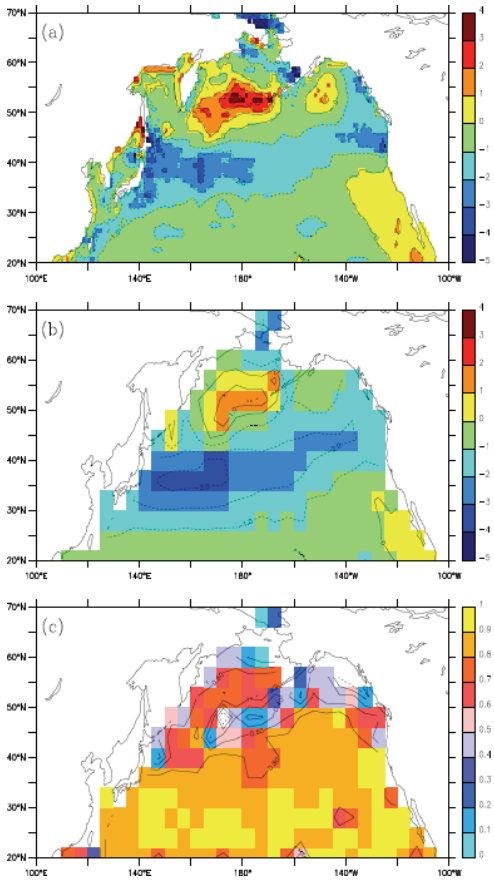

Fig. 2. Annual mean air-sea CO_2 flux from the North Pacific from **(a)** the assimilation and **(b)** Takahashi et al. (2009). Units are in mol m^{-2} yr^{-1}. **(c)** Seasonal correlation coefficients between assimilation and Takahashi et al. (2009).

BGD
8, 4239–4280, 2011

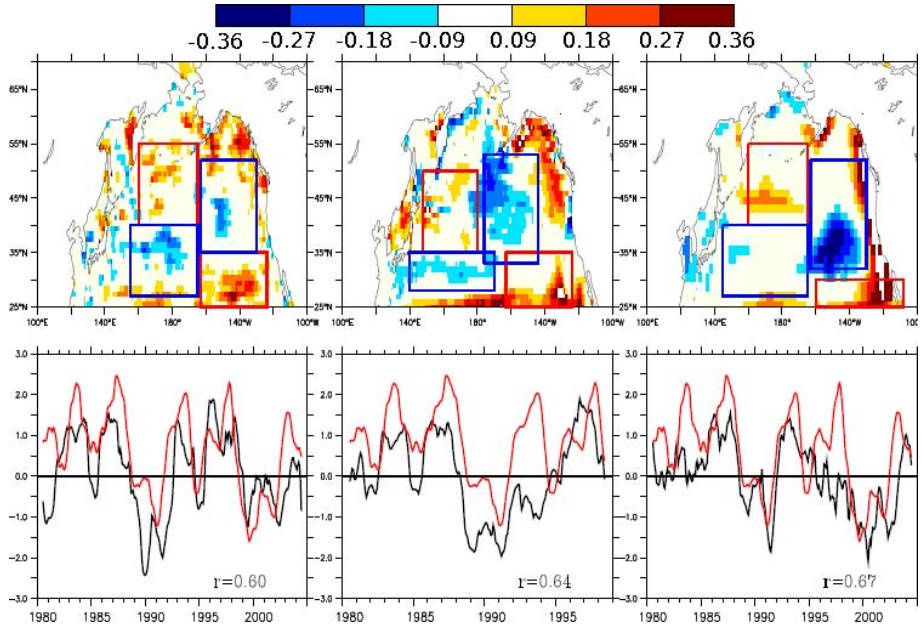

Fig. 3. (Top panels): correlation coefficients found between air-sea CO_2 flux interannual variability and PDO index from three data products such as (left) assimilation, (middle) McKinley et al. (2004) and (right) Le Quéré et al. (2005). Significant correlations above 90% level of significance are shown. (Bottom panels): CO_2 flux index corresponding to PDO from three data products (black lines) and PDO index (red lines). See text for the calculation of CO_2 flux indices. All lines are smoothed by 12-month running mean and normalized by respective standard deviations to fit into a common y-axis. The r^2 of bottom panels are of above 95% level of significance.

BGD
8, 4239–4280, 2011

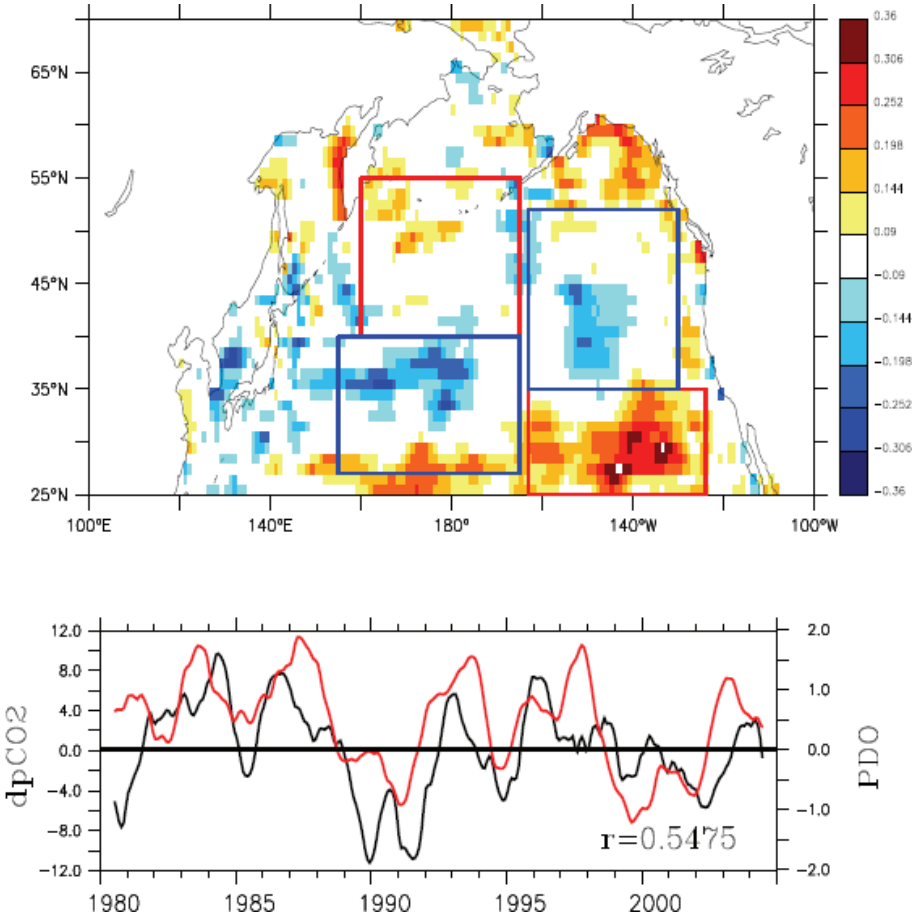

Fig. 4. (Top): correlation coefficients found between δpCO_2 interannual variability and PDO index. (Bottom): δpCO_2 index corresponding to PDO (black line) and PDO index (red line). δpCO_2 data from assimilation are used.

BGD
8, 4239–4280, 2011

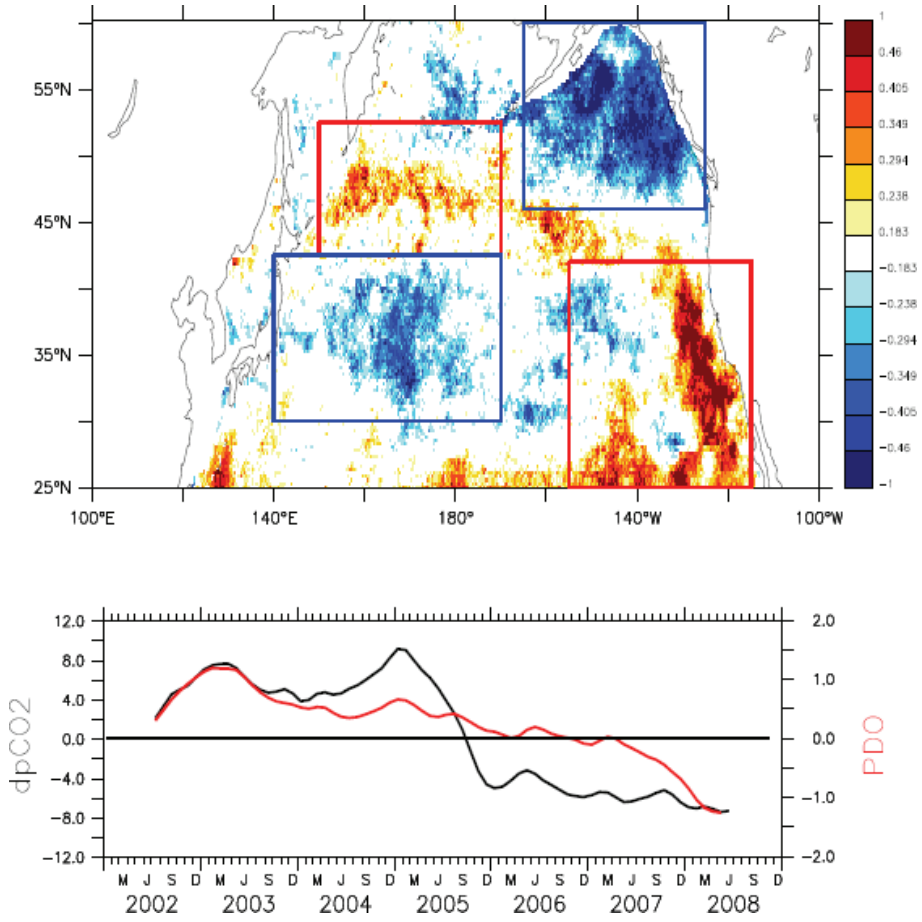

Fig. 5. Same as Fig. 4 but from Telszewski et al. (2011) pCO_2 using neural network algorithm for a period of 2002 to 2008.

BGD
8, 4239–4280, 2011

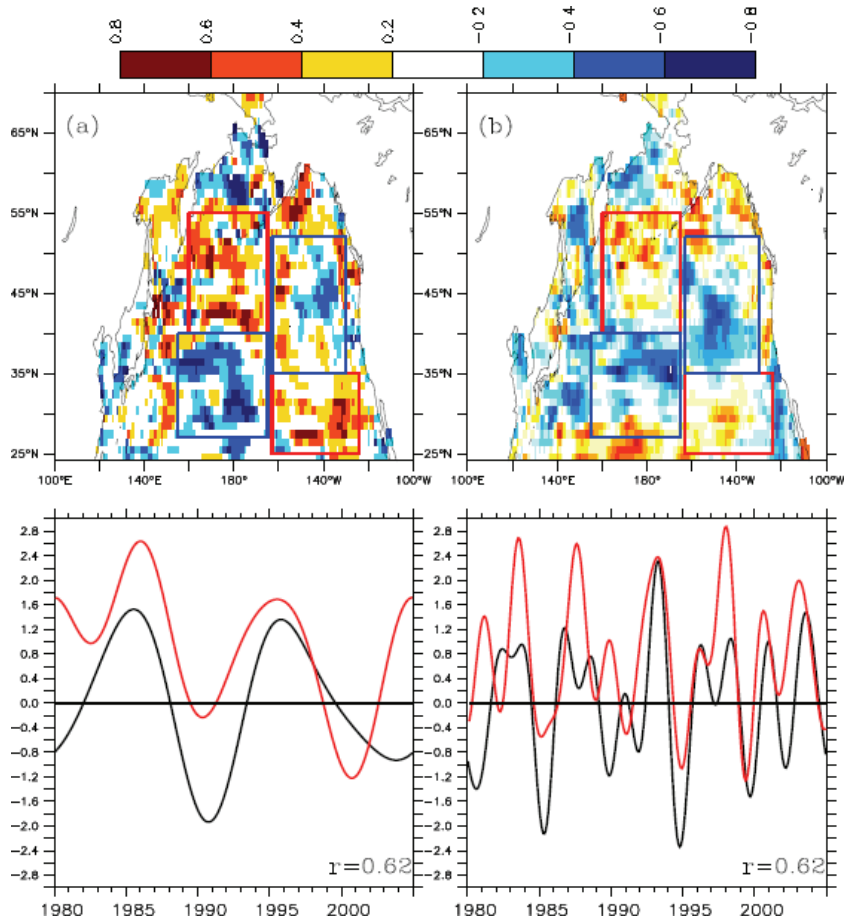

Fig. 6. Same as Fig. 3 left column but for separated components of (left) > 6.5 yr cycles and (right) < 6.5 yr cycles of CO_2 flux anomalies and PDO. CO_2 flux data from assimilation are used.

BGD
8, 4239–4280, 2011

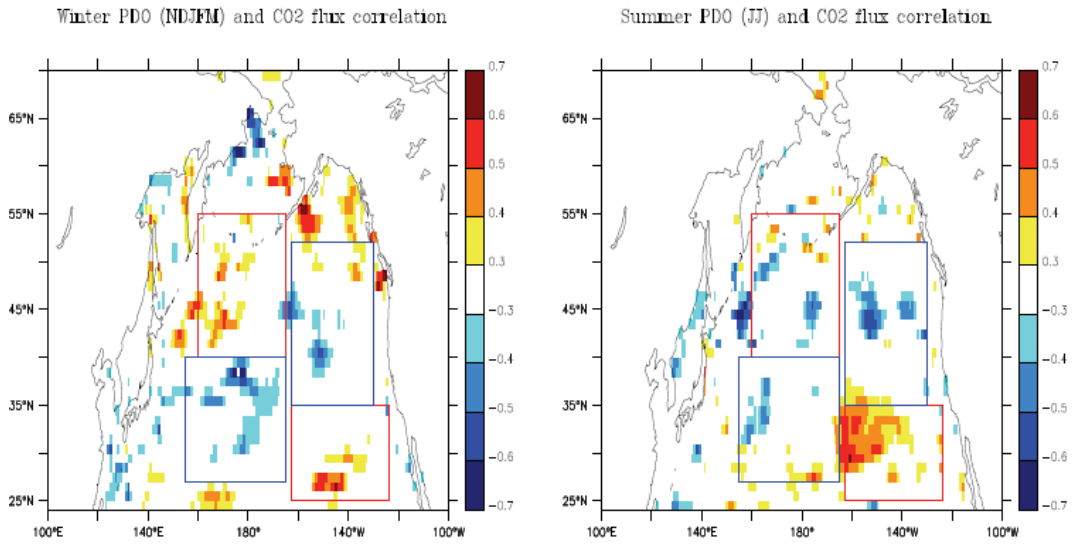

Fig. 7. Same as Fig. 3 left column but correlations are found from (left) winter months and (right) summer months CO_2 flux anomalies with corresponding PDO index.

BGD
8, 4239–4280, 2011

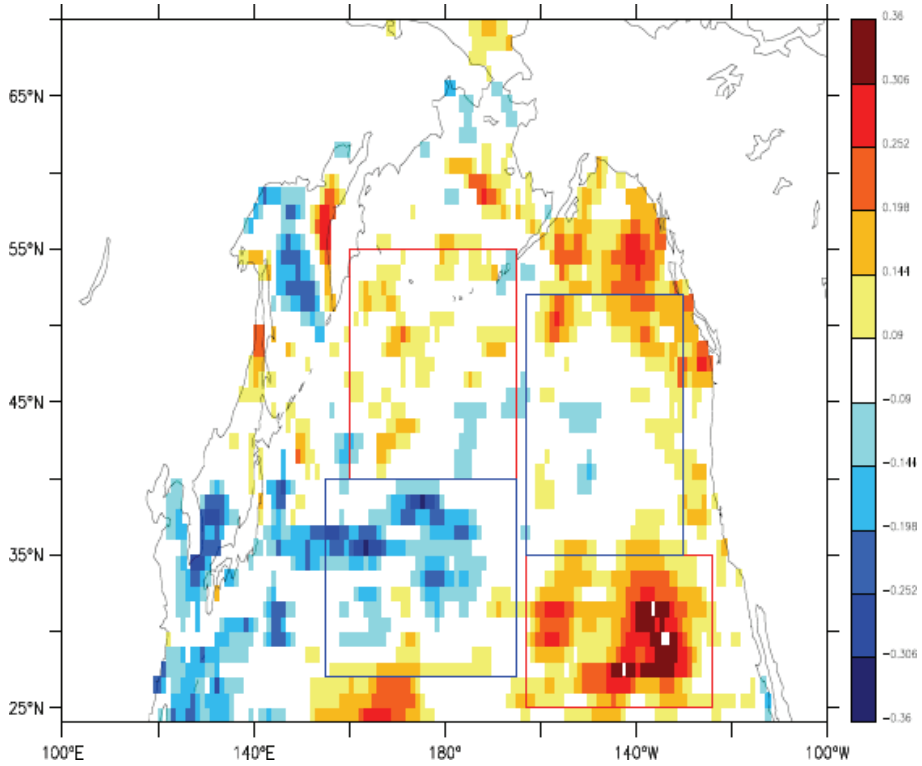

Fig. 8. Partial correlation between CO_2 flux anomalies and PDO after removing the correlations between CO_2 flux anomalies and ENSO. CO_2 flux data from assimilation are used.

BGD
8, 4239–4280, 2011

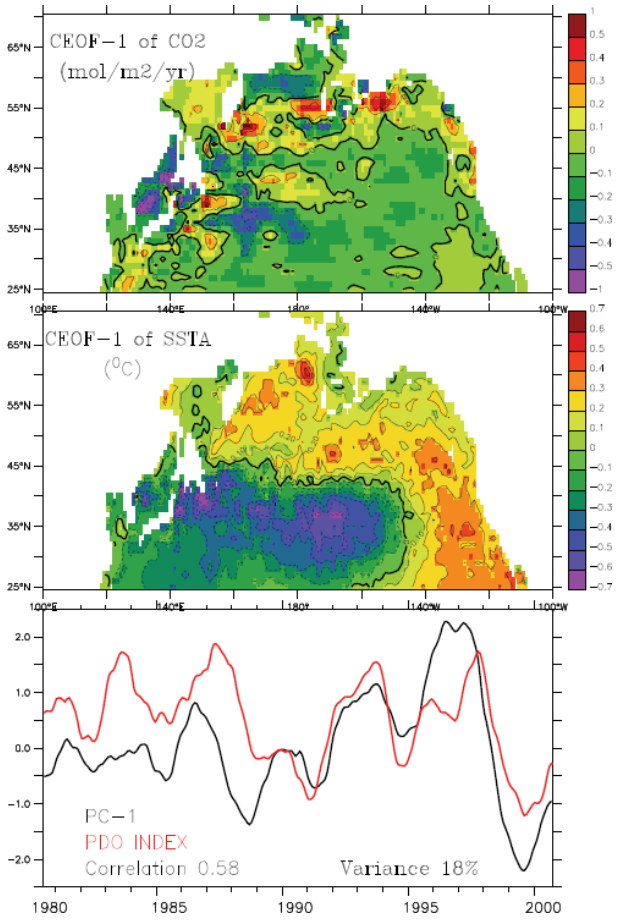

Fig. 9. (Top) CEOF-1 of CO_2 flux anomalies over the SST anomalies. (Middle) CEOF-1 of SST anomalies over CO_2 flux anomalies. (Bottom) PC-1 (black-line) and PDO (redline).

BGD
8, 4239–4280, 2011

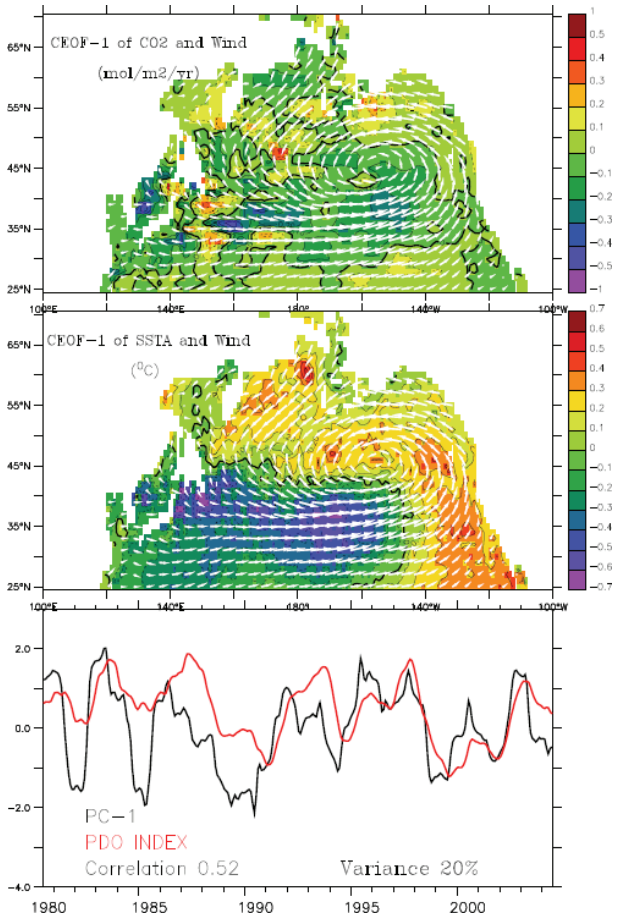

Fig. 10. Same as Fig. 9, but for CEOFs of CO_2 flux and wind stress anomalies. The middle panel is same as the middle panel of Fig. 9, but CEOF-1 wind stress vectors overlaid.

BGD
8, 4239–4280, 2011

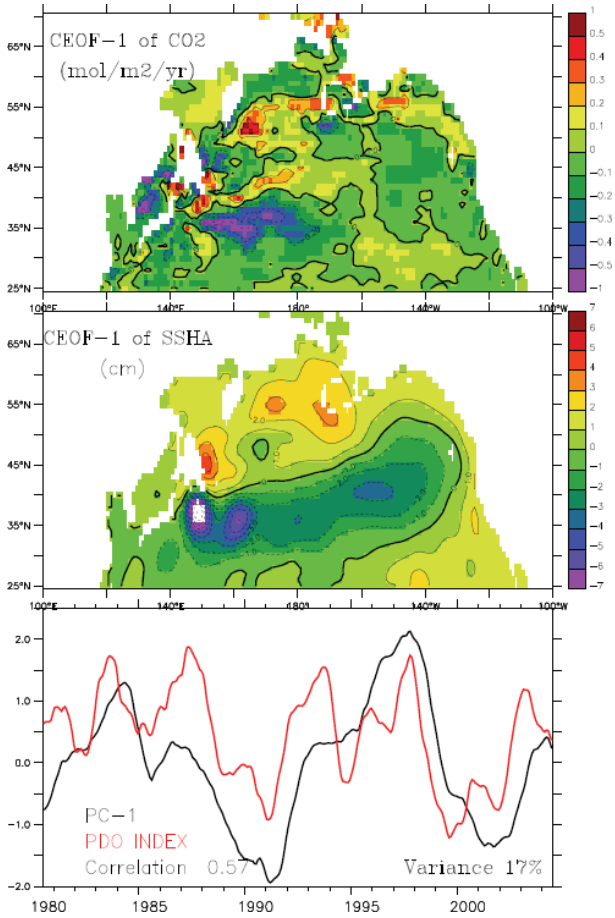

Fig. 11. Same as Fig. 9, but for CEOFs of CO_2 flux and SSH anomalies.

BGD
8, 4239–4280, 2011

Climate impacts on the structures of the North Pacific air-sea CO_2 flux variability

V. Valsala et al.

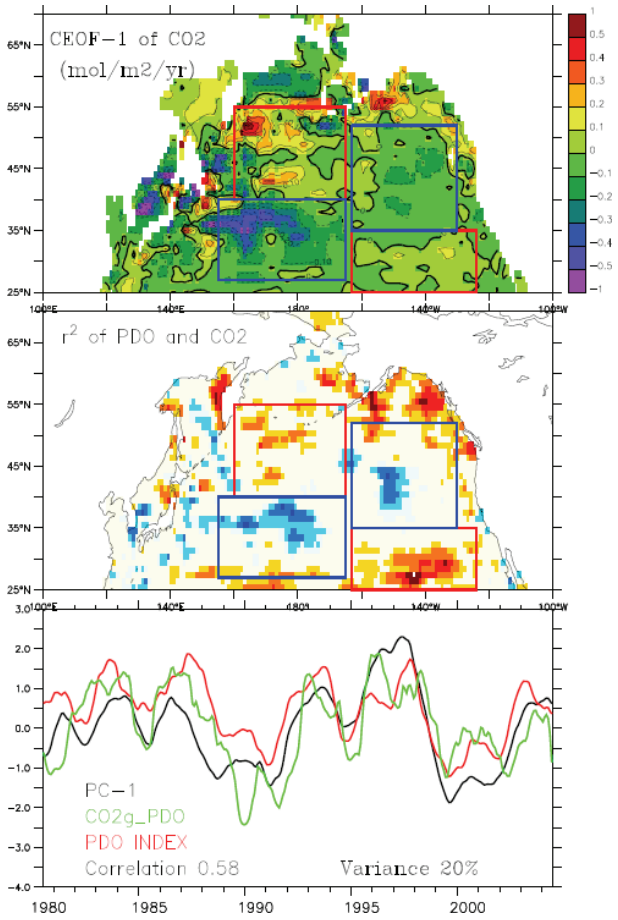

Fig. 12. (Top) CEOF of CO_2 flux with SST and SSH. (Middle) Same as top-left panel of Fig. 3. (Bottom) PC-1, CO_2g_PDO and PDO index (see Fig. 3 caption for more details).

BGD
8, 4239–4280, 2011

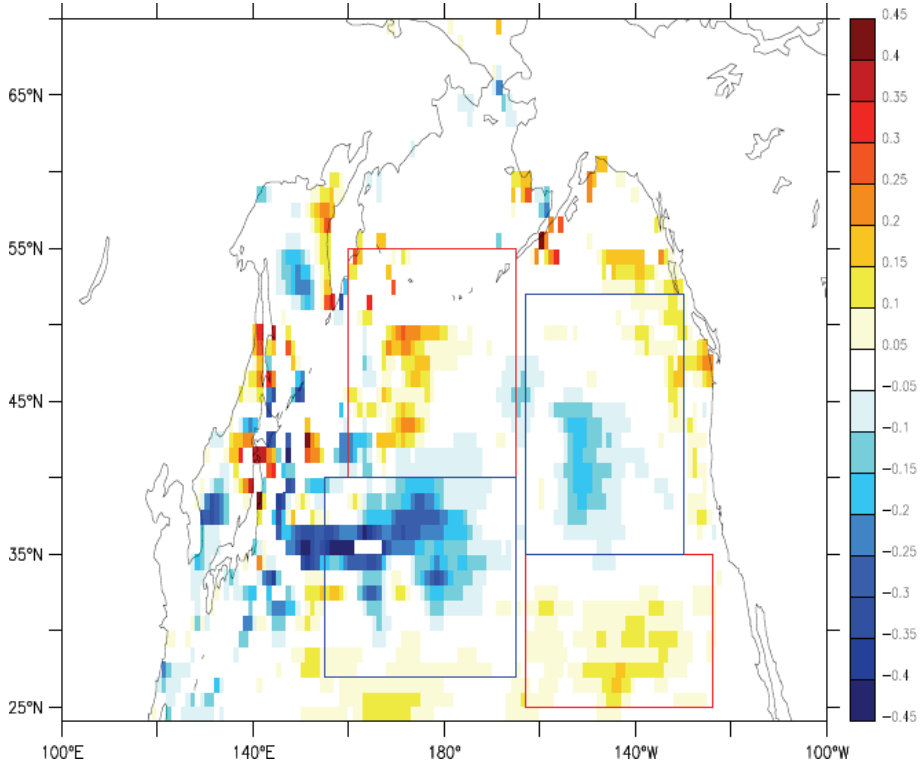

Fig. 13. Regressed CO_2 flux anomalies (mol m^{-2} yr^{-1}) over PDO.

BGD
8, 4239–4280, 2011

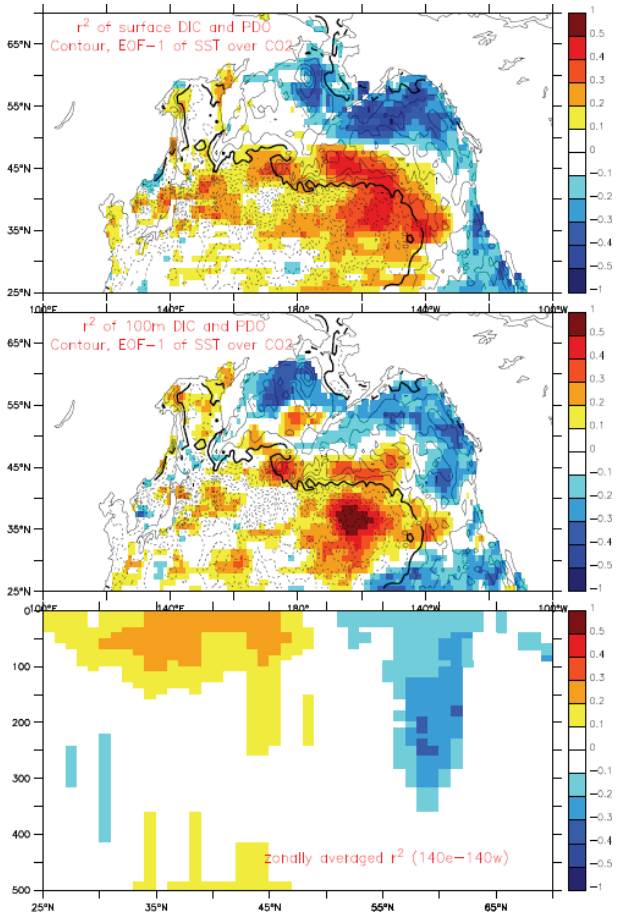

Fig. 14. Correlations between DIC and PDO shown for the (top-panel) surface and for (middle-panel) 100 m depth level. CEOF-1 of SST over CO_2 flux is overlaid as contours. Bottom panel shows the vertical section of correlations averaged over a zonal dimension of 140° E to 140° W.

BGD
8, 4239–4280, 2011

Climate impacts on the structures of the North Pacific air-sea CO_2 flux variability

V. Valsala et al.